Journal of Robotics and Control (JRC)
Volume 4, Issue 5, 2023
ISSN: 2715-5072, DOI: 10.18196/jrc.v4i5.19448

A Fuzzy LQR PID Control for a Two-Legged Wheel Robot with Uncertainties and Variant Height

Duc Thien Tran [1*], Nguyen Minh Hoang [2], Nguyen Huu Loc [3], Quoc Thanh Truong [4], Nguyen Thanh Nha [5]
[1, 2, 3, 5] Department of Automation Control, Ho Chi Minh City University of Technology and Education, Vietnam
[4] Faculty of Mechanical Engineering, Ho Chi Minh City University of Technology, Vietnam
Email: [1] thientd@hcmute.edu.vn, [2] nguyenhoangbh182@gmail.com, [3] nguyenhuuloc.0373170240@gmail.com,
[4] tqthanh@hcmut.edu.vn, [5] ntnha0639@gmail.com
*Corresponding Author

***Abstract*—This paper proposes a fuzzy LQR PID control for a two-legged wheeled balancing robot for keeping stability against uncertainties and variant heights. The proposed control includes the fuzzy supervisor, LQR, PID, and two calibrations. The fuzzy LQR is conducted to control the stability and motion of the robot while its posture changes with respect to time. The fuzzy supervisor is used to adjust the LQR control according to the robotic height. It consists of one input and one output. The input and output have three membership functions, respectively, to three postures of the robot. The PID control is used to control the posture of the robot. The first calibration is used to compensate for the bias value of the tilting angle when the robot changes its posture. The second calibration is applied to compute the robotic height according to the hip angle. In order to verify the effectiveness of the proposed control, a practical robot with the variant height is constructed, and the proposed control is embedded in the control board. Finally, two experiments are also conducted to verify the balancing and moving ability of the robot with the variant posture.**

Keywords—Fuzzy LQR Control; Two-Legged Wheeled Balancing Robot; PID Control; Fuzzy Logic System.

I. INTRODUCTION

In recent years, autonomous robots have been invented rapidly to share manpower requirements in factories, restaurants [1], airports [2], and delivery [3][4]. Unlike conventional robots and human workers operating as separate workspaces, human-robot cooperation is used to complete complex tasks. As a result, the human-robot interaction must be considered in the robot design, which means that the robots and humans can share the workspace together [5]. Two-wheel inverted pendulum (TWIP) robots [6], an extended system of inverted pendulums, and mobile robots, own advantages such as compactness, mobility, and human-like functions. This kind of robot has more applications in logistics transportation, commuting, and navigation, self-balancing capability. Because the TWIP mobile platform [7] is classified as an underactuated system that implements the 3-DOF motion of pitch, yaw, and straight movement with only two actuator inputs, high-performance motion control for this robot is a highly challenging task for the control community and recently numerous results have been reported as well-classified.

When the TWIP robots work at a small pitch angle around the balancing point, some conventional linear control techniques such as PID control [8-11] and linear quadratic regulator (LQR) [8][9][12-16] have been employed. However, when the robot operates in nonlinear regions with large pitch angles because of external disturbances, modeling errors, or internal maneuvers, the control performance of the linear control approaches will be degraded. In order to alleviate these problems and enhance the control performance, many nonlinear control methods have been investigated, such as feedback linearization control [17][18], sliding mode control [19-21], backstepping control [22-24], and model predictive control [25][26]. These approaches usually require a mathematical model for the design procedure. In practice, it is hard to determine exactly the mathematical model, parameters usually change with respect to time due to the aging and affections of the external environment. In order to handle these challenges, adaptive control [19][27-29], neural network control [19][30-32], and fuzzy control [33-36] have been investigated for the TWIP robots. In [19], a neural network was used to estimate the unknown model parameters and a robust adaptive control was applied to compensate for the estimator errors and uncertainties in a two-wheeled self-balancing robot system. In [27], an adaptive backstepping control was constructed for a wheeled inverted pendulum system under the presence of the model parameter uncertainties. In [30], an adaptive neural network was used to compensate for the unknown terms in the output dynamics of a self-balancing robot. In [33], a fuzzy logic control and a pole placement state-feedback controller were both designed for a two-wheeled self-balancing robot against the disturbance force. The pole placement state-feedback controller was used to keep the balance of the robot, and the fuzzy logic control was used to control the position of the robot. In [37], a fuzzy and PD control was applied for a two-wheeled self-balancing robot with structured and unstructured uncertainties. The PD control was used to control the balancing of the robot and the fuzzy PD control was utilized to control the position of the robot.

The conventional TWIP robots are well known moving fast and stably on a flat road. However, when they move in uneven terrain, such as gullies and slopes, their limitations appear. They cannot overcome an obstacle when the radius of the wheel is less than the height of the obstacle or the contact point is above the center of the wheel [38]. In order to manage this challenge, some advanced self-balancing robots [38-41] are constructed to work corporately with people. The study in [38] designed a terrain-adaptive two-legged wheeled robot with leg mechanisms which can jump over obstacles. Klemm et al. [39] described the fundamental design of Ascento, a

two-legged wheeled jumping robot, that moved on uneven terrain and also climbed the stairs by jumping. Zhou et al. [40] proposed a centroidal adjustment control to let the robot have higher robustness in moving. Some conventional control approaches [39][42-48] have been investigated to manage the balance and height control problems in these types of robot. In [39], a linear quadratic regulator (LQR) and PID controller were applied for the Ascento robot to control the stabilization, driving and jumping. For the stabilization and driving, the LQR controller was designed from linearization state space models linearized around ten different leg heights. In [42], a cascade PID controller was proposed for a bipedal leg-wheeled robot to guarantee the stabilization and driving. In [49], LQR controller and fuzzy PD controller were investigated on a new type of wheel legged robot with parallel four-bar mechanism for stable movement and jumping over obstacles.

Based on the above analysis, this paper presents a fuzzy LQR PID control for a two-legged wheeled robot (TLWR) for keeping stability against uncertainties and variant heights. The proposed control is designed based on the fuzzy supervisor, LQR, and PID. As a result, this approach does not require the rigor mathematical model. The fuzzy LQR, including a LQR control and a fuzzy supervisor, is utilized to control the stability and motion of the robot with the variant posture. According to the robotic height, the fuzzy supervisor will estimate the gains of the LQR control. The supervisor consists of one input and one output which have three membership functions, respectively, to three postures of the robot. The PID control is used to control the posture of the robot. In order to verify the effectiveness of the proposed control, the practical robot was constructed and the proposed control was embedded in the control board. Additionally, two experiments were also conducted to verify the balancing and moving ability of the robot. Because the sensor displacement plane is tilted according to the posture of the robot, some computations are implemented to compensate this tilting angle. The main contributions of this paper are summarized as follows:

1. A proposed control is constructed based on the fuzzy supervisor and three LQR controllers which are respectively designed according to three postures of the TLWR, low, medium and high postures. As a result, the complexity in the TLWR is reduced in the control design.
2. The effectiveness of the proposed control is verified on a practical testbench and the challenges, measuring the robotic height and compensating angles for the pitch angle in the real testbench, are also discussed in this paper.

This paper is constructed as follows: In section 2, the problem formulation of the two-legged wheeled balancing robot with variant height, including equivalent centroid calculation, TLWR Modeling, and linear state space model, is discussed. The proposed controller consisting of PID control and Fuzzy LQR control are designed in Section 3. In Section 4, some experiments are conducted in practical robot and the results of the proposed control are compared to another control. Finally, some conclusions and future works are mentioned in Section 5.

II. Description and Modeling of the Two-Legged Wheeled Robot

The structure of the self-balancing two-legged wheeled robot is presented in Fig. 1. The robotic system is equipped with a control board, an inertial measurement unit (IMU), a Zigbee module, three DC motors including encoders, and one 12V rechargeable lead-acid battery. The control board is designed as a primary controller, with the IMU being used to calculate the rate and angle of platform inclination. Additionally, the control board can drive the robotic platform's yaw control. Two motors, including encoders are installed at the feet of the robot to drive the robotic motion. Another is added in the hip to adjust the height of the robot. In order to save energy of the hip motor, torsion springs are installed in inner joints at the knees of the robot. Dead-reckoning computations are manipulated based on the information from two optical encoders mounted in the drive motors.

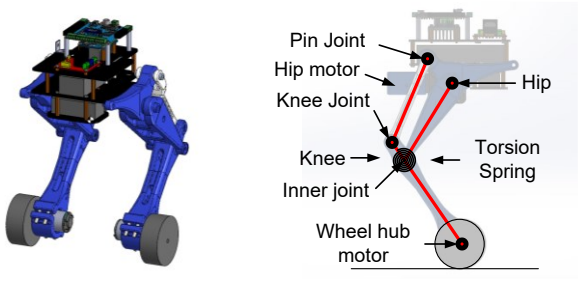

Fig. 1. The CAD model of the robot

Remark 1: In this paper, we limit the application of the upper body to sagittal motion. The yaw control of the robot is realized by the differential motion of the two wheels, and the pitch angle of the torso is controlled by the hip joint. The roll angle of the TLWR can be controlled by adjusting the height of the two legs, but in this paper, both legs perform the same motion, so the roll angle is always kept at zero. Additionally, the symbols of the TLWR utilized in this paper are summarized in Table I.

TABLE I. The Parameters of the TLWR

Symbol	Definitions
θ_w (rad)	Rotation angle of the wheel
θ_b (rad)	Tilt angle of the body of the equivalent WIP model
r	Radius of the driving wheel
I_b	Total moments of inertia of above the driving wheel in the TLWR model
l_c	Distance between the center of mass (CoM) position and wheel axis in the TLWR model
d	Distance between two wheels
m_1	Mass of the shank
m_2	Mass of the lower thigh
m_3	Mass of the upper thigh
m_4	Mass of the body
l_1	Length of the shank
l_2	Length of the lower thigh
l_3	Length of the upper thigh
l_4	Distance between the coordinate system 4th and 5th
l_5	Distance between the coordinate system 5th and 6th
τ_L	Torque of the left wheel
τ_R	Torque of the right wheel
lc_1	Position of CoM of the shank
lc_2	Position of CoM of the lower thigh
lc_3	Position of CoM of the upper thigh
lc_4	Position of CoM of the body

Symbol	Definitions
θ_1	The joint angle between the coordinate system 0th and 1th
θ_2	The joint angle between the coordinate system 1th and 2th
θ_3	The joint angle between the coordinate system 2th and 3th
θ_4	The joint angle between the coordinate system 2th and 4th
θ_5	The joint angle between the coordinate system 4th and 5th
θ_6	The joint angle between the coordinate system 5th and 6th
a	Distance between the coordinate system 2th and 3th

A. Equivalent Centroid Calculation

The coordinate systems involved in this paper are exhibited with $O_G x_G y_G z_G$ of universal frame and $O_w x_w y_w z_w$ of wheel-axle frame. In the decoupling process, the five-link multi-rigid body system is equivalent to a lumped mass point as presented in Fig. 2. The position of the equivalent centroid is weighted by the masses of the individual links and their centroid positions. To establish the relationship between this center of mass and the axle coordinate system, the Denavit–Hartenberg (D-H) convention was used to establish the kinematic model. By setting up the coordinates as presented in Fig. 3, the D-H parameters of the TLWR are shown in Table II.

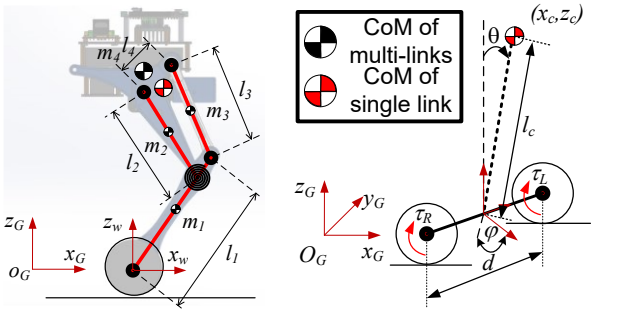

Fig. 2. Schematics of differential types of dynamic model of the robot (a) the two- legged wheeled robot, (b) The decoupled equivalent WIP model

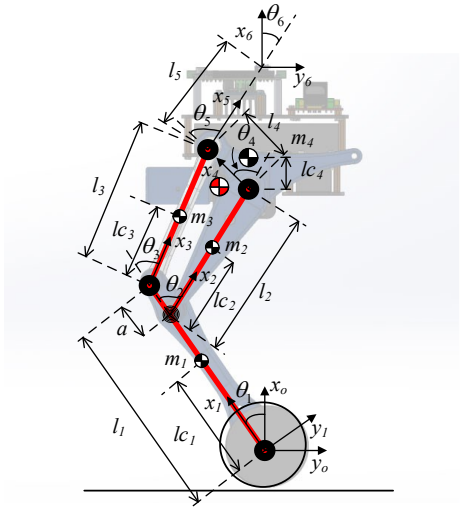

Fig. 3. Kinematic parameters of the TLWR

TABLE II. DH-PARAMETERS OF THE TLWR

Coordinate	α_{i-1}	α_{i-1}	d_i	θ_i
1	0	0	0	θ_1
2	$l_1 - a$	0	0	θ_2
3	l_2	0	0	θ_4
4	l_4	0	0	θ_5
5	l_5	0	0	θ_6

The homogeneous transformation matrix from the ith coordinate to the i-1-th coordinate is given as (1).

$$ {}^{i-1}_{i}T = \begin{bmatrix} cos\,\theta_i & -sin\,\theta_i & 0 & a_{i-1} \\ sin\,\theta_i\,cos\,\alpha_{i-1} & cos\,\theta_i\,cos\,\alpha_{i-1} & -sin\,\alpha_{i-1} & -d_i\,sin\,\alpha_{i-1} \\ sin\,\theta_i\,sin\,\alpha_{i-1} & cos\,\theta_i\,sin\,\alpha_{i-1} & cos\,\alpha_{i-1} & d_i\,cos\,\alpha_{i-1} \\ 0 & 0 & 0 & 1 \end{bmatrix} \quad (1) $$

The homogeneous transformation matrix between the coordinate system i and the axle coordinate system is as (2).

$$ {}^{w}_{i}T = {}^{w}_{1}T\,{}^{1}_{2}T \ldots {}^{i-1}_{i}T \quad (2) $$

The position of the CoM of the upper body relative to the world coordinate system can be presented as (3).

$$ {}^{w}P_C(q_b) = \frac{\sum_{i=1}^{n} m_i\,{}^{w}P_{Ci}(q_b)}{\sum_{i=1}^{n} m_i} \qquad {}^{w}P_{Ci}(q_b) = {}^{w}_{i}T(q_b)\;{}^{i}P_{Ci} \quad (3) $$

where m_i is the mass of the ith link, $q_b = [q_{b_1}, \ldots, q_{b4}]^T$ is the actual angles, ${}^{w}P_C = [x_c, z_c]^T$ is the position coordinate of the equivalent CoM relative to the axle coordinate system, ${}^{w}P_{Ci}$ is the position coordinate of the CoM of the ith link in the wheel axis coordinate system, and ${}^{i}P_{Ci}$ is the position of the CoM of the ith link in the local coordinate system. Based on the coordinate of CoM, the pendulum length lc and inclination angle θ of the inverted pendulum can be obtained as in equation (4) and (5).

$$ l_c = \sqrt{x_C^2 + z_C^2} \quad (4) $$

$$ \theta = a\,tan\left(\frac{x_c}{z_c}\right) \quad (5) $$

B. TLWR Modelling

Assumption 2: The driving wheels are subject to rolling constraints and there is no slippage between the wheel and the ground.

In this study, the pendulum length in (4) is used to analyze the dynamics of the inverted pendulum. The state variables of the wheel inverted pendulum are selected as $q_w = [x \quad \theta \quad \varphi]^T$. By using Euler Lagrange approach, the dynamic equations of the TLWR can be expressed as (6).

$$ M(q_w)\ddot{q}_w + V(q_w, \dot{q}_w) + G(q_w) + \tau_{ext} = B\tau_w \quad (6) $$

where $M(q_w) \in R^{3\times3}$, $V(q_w, \dot{q}_w) \in R^3$, and $G(q_w) \in R^3$ are respectively the inertia matrix, the Coriolis and Centripetal forces vector, the Gravitational force vector; B is the input matrix, τ_{ext} is the lumped uncertainties including the modeling error and external torque, $\tau_w = [\tau_L \quad \tau_R]^T$ is the wheel driving torques. In the differential-drive mobile robot, the input matrix is defined as $B = \begin{bmatrix} r^{-1} & -1 & \frac{d}{2r} \\ r^{-1} & -1 & -\frac{d}{2r} \end{bmatrix}^T$.

C. Linear State Space Model

In this study, three postures of the TLWR presented in Fig. 4 are considered in the control design. Its linear state space models are given as (7).

$$\begin{cases} \dot{x} = A_i x + B_i u \\ y = C_i x \end{cases} \quad (7)$$

where $x = [x \quad \theta \quad \varphi \quad \dot{x} \quad \dot{\theta} \quad \dot{\varphi}]^T \in R^{6\times1}$ is the state space, $u = \tau_w \in R^{2\times1}$ is the control input. A_i, B_i, C_i with $i = 1,2,3$ are respectively the matrices in three postures of the TLWR, which are computed as [50].

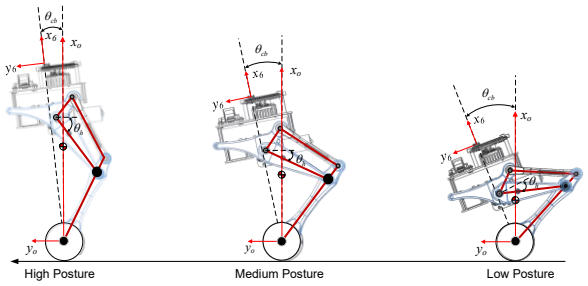

Fig. 4. Three postures of the TLWR

III. Control Design

As presented in Fig. 5, the structure of the proposed control includes the Fuzzy LQR control and Posture control. The posture control is designed from the PID control to adjust the hip angle of the robot. The height of the robot is calculated by the calibration 1 which presents the relationship between the hip angle and the height of the robot. The Fuzzy LQR control combines a fuzzy supervisor and a LQR control. The fuzzy supervisor includes one input and six outputs which are the control gains of the LQR control. The input fuzzy has three membership functions respect to the low, medium and high postures of the robot. With different postures, the center of mass of the robots are different so the dynamics of the robot is also changed. Because the control gains of LQR are dependent on the robotic dynamics, they are also different at each posture. The Fuzzy supervisor is designed to calculate the control gain of the LQR with respect to the height of the robot. When the posture of the robot changes, the inclination angle of IMU sensor also alters. As a result, inclination angles, calculated from IMU sensors, should be adjusted by the calibration 2. Based on the kinematic of the robot, the auxiliary angles are calculated with respect to the height of the robot. The input transformation matrix is used to convert the control inputs computed from the proposed control into the input voltage at each wheel motor.

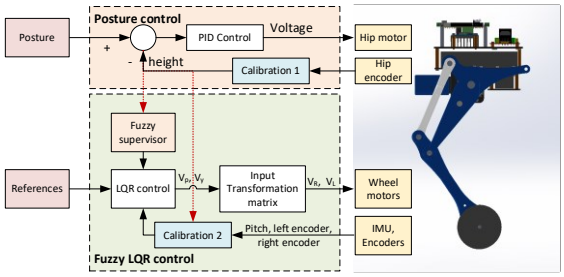

Fig. 5. Structure of the proposed control

A. PID Control

In order to control the posture of the TLWR, a PID control is used to drive the hip motor based on the difference of the posture profile and the real posture of the TLWR. Based on the geometric structure of the TLWR in Fig. 3, the pendulum length can be calculated following the hip angle. The calibration 1 is utilized to compute the robotic height according to hip angle. The PID control law is presented as (8).

$$u(t) = K_p e(t) + K_i \int_0^t e(\tau)d\tau + K_d \frac{de(t)}{dt} \quad (8)$$

where K_p is a proportional gain, K_i is an integral gain and K_d is a differential gain.

B. Linear Quaratic Regulator(LQR)

In the LQR controller, the optimal control gains, K, are computed based on the cost function (J), which optimize states, $x(t)$ and control signal, $u(t)$ of the systems (9). The control signal, $u(t)$, and the cost function, J, are selected as in (9) and (10).

$$u(t) = -Kx(t) \quad (9)$$

$$J = \frac{1}{2}\int_0^\infty \left(x^T(t)Qx(t) + u^T(t)Ru(t)\right)dt \quad (10)$$

where Q and R are positive semi-defined matric. In order to minimize the cost function, J, the control gain, K, is given as (11).

$$K = R^{-1}B^T P \in R^{2\times6} \quad (11)$$

where P is solution of the differential equation of Riccati as (12).

$$PA + A^T - PBR^{-1} + Q = 0 \quad (12)$$

Remark 2: The LQR controller performance is dependent on the selection of weight matrices and linearization matrices, A and B. As a result, different postures will give different optimal control gains, K_1, K_2 and K_3 in the low, medium and high postures, respectively.

Remark 3: When the height of the TLWR changes respect to the posture, the sensor plane will be titled at an angle correspondingly. The calibration 2 is used to compensate this titling angle of the sensor. The equation in the calibration 2 is calculated by applying the algebraic solution technique. The transformation matrix between the 6th coordination system and the origin coordination can be calculated from equation (13).

$${}^0_6T = {}^0_1T(\theta_1){}^1_2T(\theta_2)\ldots{}^4_5T(\theta_5){}^5_6T(\theta_6) = \begin{bmatrix} r_{11} & r_{12} & r_{13} & P_x \\ r_{21} & r_{22} & r_{23} & P_y \\ r_{31} & r_{23} & r_{33} & P_z \\ 0 & 0 & 0 & 1 \end{bmatrix} \quad (13)$$

By implementing some manipulations, transformation matrix, ${}^0_6T$, will only depend on the hip angle. Because the height of two legs is adjusted simultaneously, the orientation matrix of the transformation matrix, ${}^0_6T$, is a rotation operation around the z-axis. As a result, this matrix can be presented as (14).

$${}^0_6T = \begin{bmatrix} \cos(\theta_{comp}) & -sin(\theta_{comp}) & 0 & {}^0P_x \\ sin(\theta_{comp}) & \cos(\theta_{comp}) & 0 & {}^0P_y \\ 0 & 0 & 1 & {}^0P_z \\ 0 & 0 & 0 & 1 \end{bmatrix} \quad (14)$$

The compensation angle for the sensor is calculated as (15).

$$\theta_{comp} = acr\ tan\left(\frac{r_{21}}{r_{11}}\right) \quad (15)$$

The output of the calibration is presented as (16).

$$\theta_p = \theta_{p\_raw} + \theta_{comp} \quad (16)$$

C. Fuzzy Supervisor

According to the robotic height estimated from the hip angles, the fuzzy supervisor will compute the control gains in the LQR, respectively. Fig. 6 presents the structure of the fuzzy supervisor, which includes an input and 8 outputs, control gains of the LQR. Three membership functions in the input are presented as Low, Medium and High in Fig. 7.

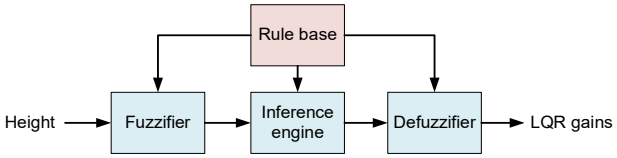

Fig. 6. Structure of the fuzzy supervisor

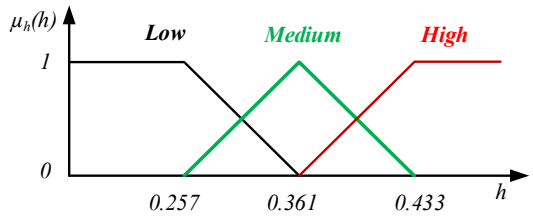

Fig. 7. Input membership function of the fuzzy supervisor

Fuzzy rules of the fuzzy supervisor are given as follows:

- If h is *Low* then $\boldsymbol{K} = \boldsymbol{K}_1$,
- If h is *Medium* then $\boldsymbol{K} = \boldsymbol{K}_2$,
- If h is *High* then $\boldsymbol{K} = \boldsymbol{K}_3$.

Where h is the height of the robot; $\boldsymbol{K}_{i(i=1,2,3)}$ are control gains of the low, medium and high postures, respectively.

The MAX – PROD aggregation method and "centroid" defuzzification method are utilized. The control gains can be computed in (17).

$$\boldsymbol{K} = \frac{mf_{low}(h)\boldsymbol{K}_1 + mf_{Medium}(h)\boldsymbol{K}_2 + mf_{High}(h)\boldsymbol{K}_3}{mf_{low}(h) + mf_{Medium}(h) + mf_{High}(h)} \quad (17)$$

IV. Experiment Discussion

A. Test Bench Description

The practical TLWR robot shown in Fig. 8 includes a board Control, two-wheel motors with encoders, a hip motor, a hip encoder, and an IMU sensor. The control board developed form ATmega2560 is used to control the stability, posture and motion of the robot. Two-wheel motors are two DC motors, JGB37-520 with the speed of 333 revolution per minute (RPM), which are attached to incremental encoder with 11 pulses per revolution (PPR). Based on the control signals which are generated from the control board, they will keep the robot stable or drive the motion of the robot. In order to adjust the posture of the robot, a high torque 5840-31ZT motor and an encoder AMT332D-V are mounted in the hip. The IMU sensor, MPU9250, is utilized to compute the titling of the robot. The power of the whole system is supplied by a 12 V lithium battery. After practical measurements, the weight of the robot is 3.15 kg, and the battery life is about 2.5 h.

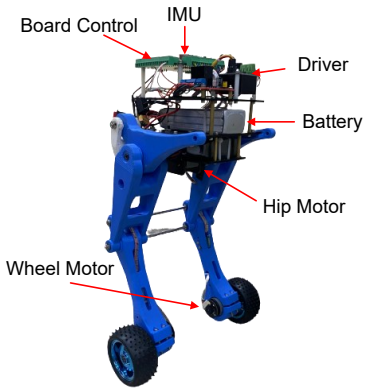

Fig. 8. Two- legged wheeled robot can change height in practice

The hardware connection diagram of the test bench is shown in Fig. 9. A graphic user interface, built by Visual studio C# on a laptop, acquires the robotic position, pitch, hip and yaw angles and control signals, and send the control gains to the robot through wireless communication in real-time through radio frequency (RF) transceiver, Zigbee C2530. The control board is constructed to conduct the proposed control from the information acquiring from IMU sensor and encoders. After the control signals are computed by the control board, they will be provided to the drivers of the hip motor and leg motor.

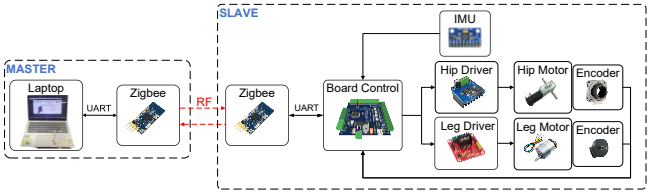

Fig. 9. Hardware connection diagram

Remark 4: The parameters of the TLWR, such as lengths, masses, moments inertia, and radius of wheels, in Table III are specified and calculated by using the mass properties in the SOLIDWORK.

TABLE III. Parameters of the Two-Legged Wheeled Robot

Symbol	Value	Unit	Symbol	Value	Unit
a	0.035	m	l_2	0.145	m
r	0.0425	m	l_3	0.145	m
d	0.276	m	l_4	0.055	m
m_1	0.56	kg	l_5	0.09275	m
m_2	0.44	kg	lc_1	0.09636	m
m_3	0.19	kg	lc_2	0.07251	m
m_4	1.96	kg	lc_3	0.07251	m
l_1	0.19	m	lc_4	0.028	m

Remark 5: In this study, the proposed control is carried out on the practical two-legged wheeled robot. The steps taken in this study are summarized as follows: Step 1 selects devices from the requirements; Step 2 designs a two-legged wheeled robot; Step 3 constructs a real model; Step 4 evaluates the performances of the actuators, sensors and mechanical structure; Step 5 conducts the LQR controllers

with different postures on the practical mode; Finally, step 6 implements the proposed control on the robot.

B. Experimental Description

In order to verify the effectiveness of the proposed control, it is compared with a Fuzzy LQR control which is designed with two membership functions in the fuzzy supervisor named as fuzzy LQR control with two membership functions (FLQR with TMF). This control is designed based on the LQR controllers in the high and low postures. The control parameters of the PID and LQR control in the postures are shown in Table IV.

TABLE IV. CONTROL PARAMETERS

Controller	Parameters
PID	$K_P = 40, K_I = 3, K_D = 0.02$
LQR Low	$\boldsymbol{K}_1 = \begin{bmatrix} 12.6 & 18.3 & 680 & 276 & 24 & 47 \\ 12.6 & 18.3 & 680 & 276 & -24 & -47 \end{bmatrix}$
LQR Medium	$\boldsymbol{K}_2 = \begin{bmatrix} 13.5 & 19.5 & 700 & 286 & 26 & 50 \\ 13.5 & 19.5 & 700 & 286 & -26 & -50 \end{bmatrix}$
LQR High	$\boldsymbol{K}_3 = \begin{bmatrix} 14.12 & 22 & 756 & 296 & 28 & 53 \\ 14.12 & 22 & 756 & 296 & -28 & -53 \end{bmatrix}$

Remark 6: Because the balancing of the robot cannot be remained during the posture of the robot change, when only the LQR in low, medium, high postures are applied independently. The fuzzy LQR control with two membership functions in fuzzy supervisor is used for comparison.

To evaluate the balancing and moving performances of the proposed controller with robot, two experiments are carried out with different scenarios to evaluate the superiority of the proposed control. In the first experiment, the robot keeps balancing in place while its height changes from high to low and from low to high during 60 seconds. In the second scenario, the robot keeps balancing, moving forward and backward, and changing its posture simultaneously during 60 seconds. The posture of the robot changes respect to time, which is illustrated in Fig. 10.

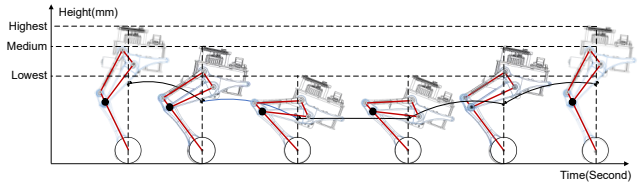

Fig. 10. Posture adjustments of the two-legged wheeled robot

C. Experiment Results

In the first scenario, the experiment is conducted to verify of the proposed control in keeping the balancing of the robot with variant postures. The robot will stay in the high posture in the initially. Its posture will change to the low posture from 15th second to 25th second. Then this status will be kept in 15 seconds after it changes to the high posture again from 40th to 50th second. Finally, the robot will stay in this posture in the last time. During the posture of the robot changes, the robot is kept balancing in place. Fig. 11 shows the output responses of the robot, which are the robot position, pitch angle, rotation angle and the height of the robot with the black lines of the reference, blue lines of the FLQR with TMF and the red lines of the proposed control. The results show that two controllers keep the robot balancing well when the posture changes with respect to time. Additionally, the proposed control with fuzzy supervisor which is designed from the controllers of the LQR controllers in three postures gives better performance than the controller with the fuzzy supervisor designed from two LQR controllers in the high and low postures Fig. 12 presents error performances of the robot, which are the robot position, pitch angle, rotation angle and the height of the robot with the blue lines of the FLQR with TMF and the red lines of the proposed control. Fig. 13 presents the control signals of the controllers in the left, right and hip motor with the blue lines of the FLQR with TMF and the red lines of the proposed control. The chattering effect in the motors is significant.

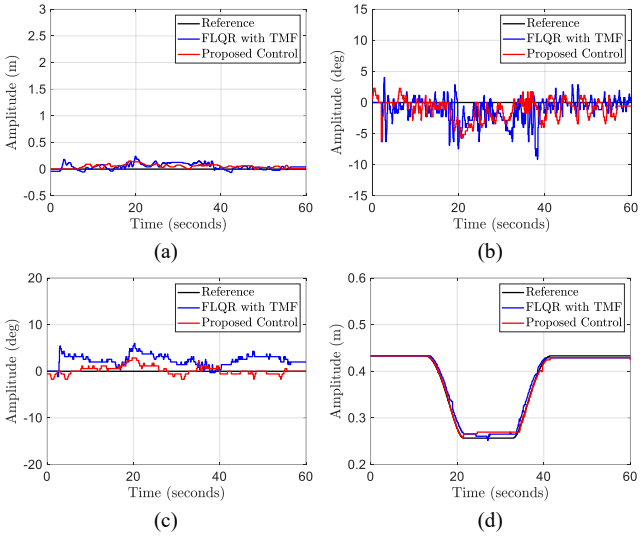

Fig. 11. Output response of the two-legged wheeled robot with two controllers in (a) robot position; (b) pitch angle; (c) rotation angle; (d) height of robot

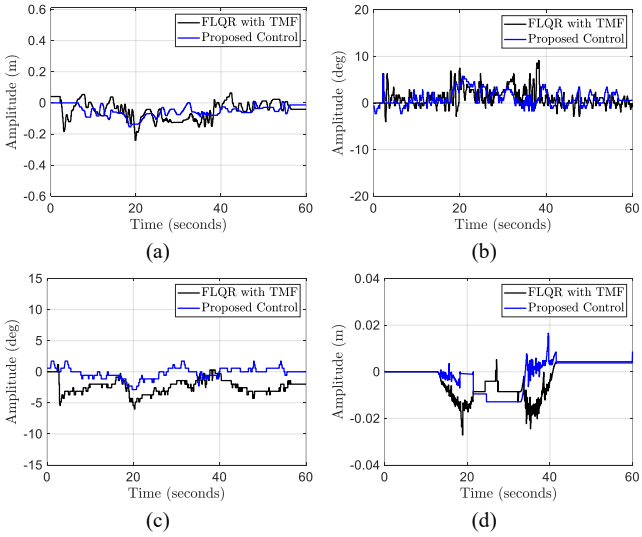

Fig. 12. Error performance of two controllers in (a) robot position; (b) pitch angle; (c) rotation angle; (d) height of robot

In the second scenario, the experiment is implemented to evaluate the effectiveness of the proposed control in keeping the balancing of the robot with variant postures when the robot moves forward and backward. The robot will stay in the high posture in the initial time, then it will begin decreasing its height to the low posture from the 10th to the 20th second. It will stay the low posture in 15 seconds and increase the height to high posture from the 35th to the 45th second.

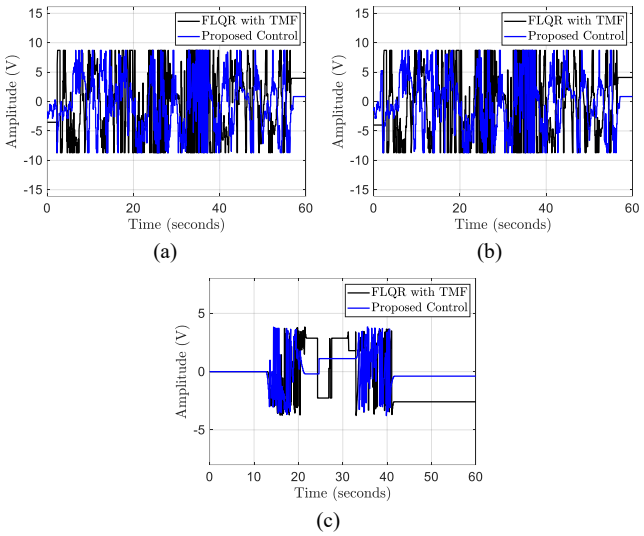

Fig. 13. Control signals response of the two-legged wheeled robot with two controllers in (a) left motor; (b) right motor; (c) hip motor

Finally, it will keep this status in the last time. Besides the posture change with respect to time, the robot also moves forward to the setpoint of 1.6 meter from the origin position from the the 10th to the 20th second. Then, it stays in this place in 15 seconds before moving backward to the origin position from the 35th to the 45th second.

Finally, it will stay at the origin position in the last time. Fig. 14 shows the output responses of the robot, which are the robot position, pitch angle, rotation angle and the height of the robot with the black lines of the reference, blue lines of the FLQR with TMF and the red lines of the proposed control. The results show that two controllers keep the robot balancing well when the robot moves forward and backward with variant postures.

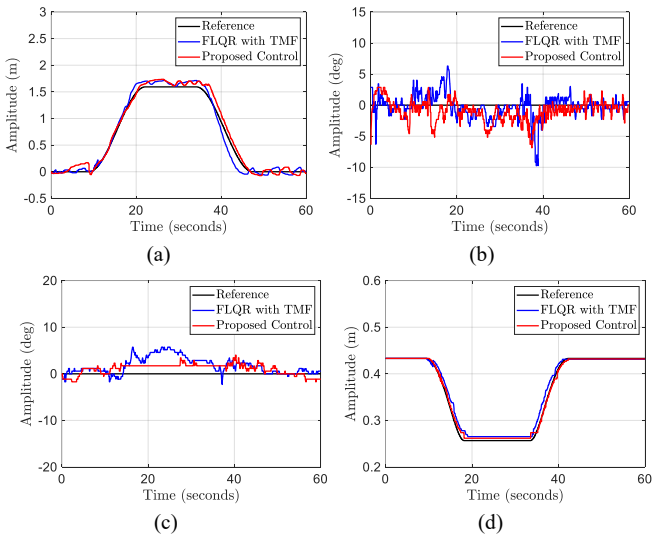

Fig. 14. Output response of the two-legged wheeled robot with two controllers in (a) robot position; (b) pitch angle; (c) rotation angle; (d) height of robot

Additionally, the proposed control with fuzzy supervisor gives better performance than the FLQR with TMF. Fig. 15 presents error performances of the robot, which are the robot position, pitch angle, rotation angle and the height of the robot with the blue lines of the FLQR with TMF and the red lines of the proposed control Fig. 16 presents the control signals of the controllers in the left, right and hip motor with the blue lines of the FLQR with TMF and the red lines of the proposed control. The chattering effect in the motors is also significant in this case study.

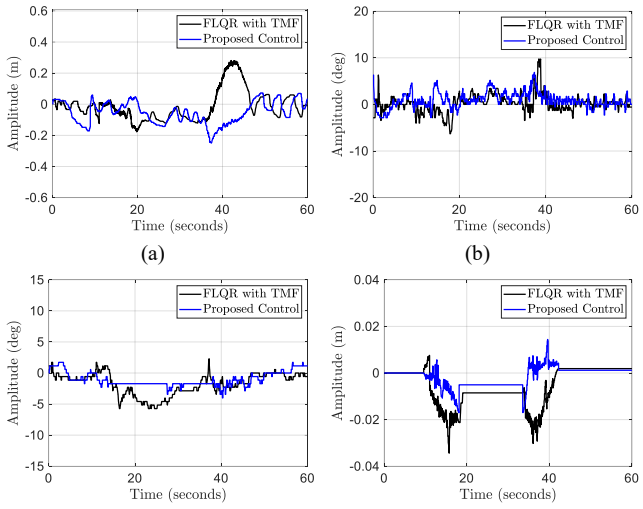

Fig. 15. Error performance of two controllers in (a) robot position; (b) pitch angle; (c) rotation angle; (d) height of robot

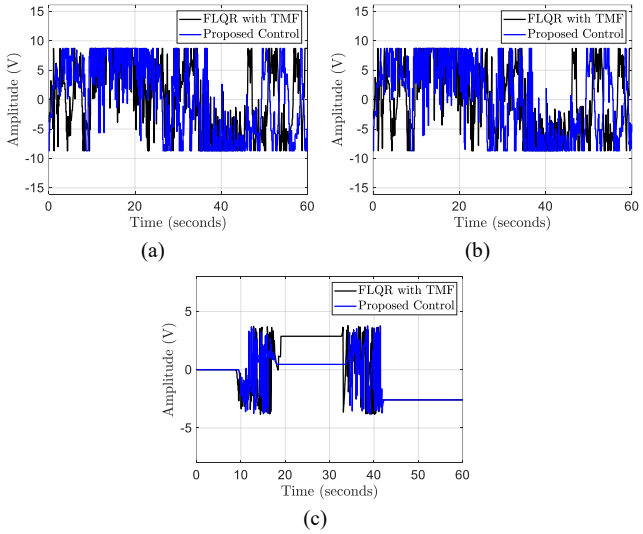

Fig. 16. Control signals response of the two-legged wheeled robot with two controllers (a) left motor; (b) right motor; and (c) hip motor

V. Conclusion and Future Work

This paper presented a fuzzy LQR PID control for a two-legged wheeled balancing robot for keeping its stability against the uncertainties and variant heights. The proposed control includes the fuzzy supervisor, LQR, and PID. The fuzzy LQR is conducted to control the stability and motion of the robot with the variant postures. The fuzzy supervisor is used to adjust the LQR control according to the robotic height. It consists of one input and one output. The input and output have three membership functions respectively to three postures of the robot. The PID control is used to control the posture of the robot. In order to verify the effectiveness of the proposed control, the practical robot was constructed and the proposed control were embedded in the control board. Two experiments were also conducted to verify the balancing and

moving ability of the robot. In practice, when the posture of robot changes, the sensor mounting plane is tilting an angle with respect to the height of the robot. So, a calibration was carried out to compensate with the pitch angle which is computed from the IMU sensor.

Future works in this study will focus on; 1) Suppressing chattering effect; 2) improving the robotic test bench to control the length of two legs separately; 3) applying type-2 fuzzy system to manage the uncertainties in the system; 4) Investigating some advance navigation methods by using Lidar and CCD images.

ACKNOWLEDGEMENT

The research topic was supported by The Youth Incubator for Science and Technology Programme, managed by Youth Promotion Science and Technology Center - Ho Chi Minh Communist Youth Union and Department of Science and Technology of Ho Chi Minh City, the contract number is " 22/2022/ HĐ-KHCNT-VU" signed on 30th, December, 2022.

REFERENCES

[1] S. Harapanahalli, N. O. Mahony, G. V. Hernandez, S. Campbell, D. Riordan, and J. Walsh, "Autonomous Navigation of mobile robots in factory environment," *Procedia Manufacturing*, vol. 38, pp. 1524-1531, 2019.

[2] D. Di Paola, D. Naso, A. Milella, G. Cicirelli, and A. Distante, "Multi-sensor surveillance of indoor environments by an autonomous mobile robot," *International Journal of Intelligent Systems Technologies and Applications*, vol. 8, no. 1-4, pp. 18-35, 2010, doi: 10.1504/IJISTA.2010.030187.

[3] S. Srinivas, S. Ramachandiran, and S. Rajendran, "Autonomous robot-driven deliveries: A review of recent developments and future directions," *Transportation Research Part E: Logistics and Transportation Review*, vol. 165, p. 102834, 2022.

[4] C. H. G. Li, L. P. Zhou, and Y. H. Chao, "Self-Balancing Two-Wheeled Robot Featuring Intelligent End-to-End Deep Visual-Steering," *IEEE/ASME Transactions on Mechatronics*, vol. 26, no. 5, pp. 2263-2273, 2021, doi: 10.1109/TMECH.2020.3036579.

[5] W. Bauer, M. Bender, M. Braun, P. Rally, and O. Scholtz, "Lightweight robots in manual assembly–best to start simply," *Frauenhofer-Institut für Arbeitswirtschaft und Organisation IAO, Stuttgart*, vol. 1, 2016.

[6] H. W. Kim and S. Jung, "Fuzzy logic application to a two-wheel mobile robot for balancing control performance," *International Journal of Fuzzy Logic and Intelligent Systems*, vol. 12, no. 2, pp. 154-161, 2012.

[7] S. Kim and S. Kwon, "Nonlinear Optimal Control Design for Underactuated Two-Wheeled Inverted Pendulum Mobile Platform," *IEEE/ASME Transactions on Mechatronics*, vol. 22, no. 6, pp. 2803-2808, 2017, doi: 10.1109/TMECH.2017.2767085.

[8] K. V. Chate García, O. E. Prado Ramírez, and C. F. Rengifo Rodas, "Comparative analysis between fuzzy logic control, lqr control with kalman filter and pid control for a two wheeled inverted pendulum," in *Advances in Automation and Robotics Research in Latin America: Proceedings of the 1st Latin American Congress on Automation and Robotics*, pp. 144-156, 2017.

[9] A. A. Bature, S. Buyamin, M. N. Ahmad, and M. Muhammad, "A comparison of controllers for balancing two wheeled inverted pendulum robot," *International Journal of Mechanical & Mechatronics Engineering*, vol. 14, no. 3, pp. 62-68, 2014.

[10] N. G. M. Thao, D. H. Nghia, and N. H. Phuc, "A PID backstepping controller for two-wheeled self-balancing robot," *International Forum on Strategic Technology 2010*, pp. 76-81, 2010, doi: 10.1109/IFOST.2010.5668001.

[11] T. Nikita and K. T. Prajwal, "PID Controller Based Two Wheeled Self Balancing Robot," *2021 5th International Conference on Trends in Electronics and Informatics (ICOEI)*, pp. 1-4, 2021, doi: 10.1109/ICOEI51242.2021.9453091.

[12] F. Sun, Z. Yu, and H. Yang, "A design for two-wheeled self-balancing robot based on Kalman filter and LQR," in *2014 International Conference on Mechatronics and Control (ICMC)*, pp. 612-616, 2014, doi: 10.1109/ICMC.2014.7231628.

[13] J. Fang, "The LQR Controller Design of Two-Wheeled Self-Balancing Robot Based on the Particle Swarm Optimization Algorithm," *Mathematical Problems in Engineering*, vol. 2014, p. 729095, 2014, doi: 10.1155/2014/729095.

[14] H. F. Murcia and A. E. González, "Performance comparison between PID and LQR control on a 2-wheel inverted pendulum robot," in *2016 IEEE Colombian Conference on Robotics and Automation (CCRA)*, pp. 1-6, 2016, doi: 10.1109/CCRA.2016.7811420.

[15] C. Xu, M. Li, and F. Pan, "The system design and LQR control of a two-wheels self-balancing mobile robot," in *2011 International Conference on Electrical and Control Engineering*, pp. 2786-2789, 2011, doi: 10.1109/ICECENG.2011.6057680.

[16] M. Muhammad, S. Buyamin, M. N. Ahmad, S. Nawawi, and A. Bature, "Multiple Operating Points Model-Based Control of a Two-Wheeled Inverted Pendulum Mobile Robot," *International Journal of Mechanical & Mechatronics Engineering*, vol. 13, pp. 1-9, 2013.

[17] A. I. Glushchenko, K. A. Lastochkin, and V. A. Petrov, "Development of Two-Wheeled Balancing Robot Optimal Control System based on Its Feedback Linearization," in *2019 International Multi-Conference on Industrial Engineering and Modern Technologies (FarEastCon)*, pp. 1-6, 2019, doi: 10.1109/FarEastCon.2019.8934245.

[18] J. Kedzierski and K. Tchoń, "Feedback Control of a Balancing Robot," *IFAC Proceedings Volumes*, vol. 42, no. 13, pp. 495-500, 2009.

[19] V. B. V. Nghia, T. Van Thien, N. N. Son, and M. T. Long, "Adaptive neural sliding mode control for two wheel self balancing robot," *International Journal of Dynamics and Control*, vol. 10, no. 3, pp. 771-784, 2022, doi: 10.1007/s40435-021-00832-1.

[20] S. Yuan, G. Lei, and X. Bin, "Dynamic modeling and sliding mode controller design of a two-wheeled self-balancing robot," in *2016 IEEE International Conference on Mechatronics and Automation*, pp. 2437-2442, 2016, doi: 10.1109/ICMA.2016.7558948.

[21] M. Hou, X. Zhang, D. Chen, and Z. Xu, "Hierarchical Sliding Mode Control Combined with Nonlinear Disturbance Observer for Wheeled Inverted Pendulum Robot Trajectory Tracking," *Applied Sciences*, vol. 13, no. 7, p. 4350, 2023.

[22] E. Ahmad, A. U. Rehman, O. Khan, M. Haseeb, and N. Ali, "Backstepping control design for two-wheeled self balancing robot," in *2018 1st International Conference on Power, Energy and Smart Grid (ICPESG)*, pp. 1-6, 2018, doi: 10.1109/ICPESG.2018.8384494.

[23] N. Esmaeili, A. Alfi, and H. Khosravi, "Balancing and Trajectory Tracking of Two-Wheeled Mobile Robot Using Backstepping Sliding Mode Control: Design and Experiments," *Journal of Intelligent & Robotic Systems*, vol. 87, no. 3, pp. 601-613, 2017, doi: 10.1007/s10846-017-0486-9.

[24] A. J. Humaidi *et al*., "Algorithmic Design of Block Backstepping Motion and Stabilization Control for Segway Mobile Robot," in *Mobile Robot: Motion Control and Path Planning*, pp. 557-607, 2023.

[25] S. Sekiguchi, A. Yorozu, K. Kuno, M. Okada, Y. Watanabe, and M. Takahashi, "Human-friendly control system design for two-wheeled service robot with optimal control approach," *Robotics and Autonomous Systems*, vol. 131, p. 103562, 2020.

[26] M. M. Azimi and H. R. Koofigar, "Model predictive control for a two wheeled self balancing robot," in *2013 First RSI/ISM International Conference on Robotics and Mechatronics (ICRoM)*, pp. 152-157, 2013, doi: 10.1109/ICRoM.2013.6510097.

[27] R. Cui, J. Guo, and Z. Mao, "Adaptive backstepping control of wheeled inverted pendulums models," *Nonlinear Dynamics,* vol. 79, no. 1, pp. 501-511, 2015, doi: 10.1007/s11071-014-1682-9.

[28] W. Sun, S. F. Su, J. Xia, and Y. Wu, "Adaptive Tracking Control of Wheeled Inverted Pendulums With Periodic Disturbances," *IEEE Transactions on Cybernetics*, vol. 50, no. 5, pp. 1867-1876, 2020, doi: 10.1109/TCYB.2018.2884707.

[29] C. Yang, Z. Li, and J. Li, "Trajectory Planning and Optimized Adaptive Control for a Class of Wheeled Inverted Pendulum Vehicle Models," *IEEE Transactions on Cybernetics*, vol. 43, no. 1, pp. 24-36, 2013, doi: 10.1109/TSMCB.2012.2198813.

[30] I. Gandarilla, J. Montoya-Cháirez, V. Santibáñez, C. Aguilar-Avelar, and J. Moreno-Valenzuela, "Trajectory tracking control of a self-balancing robot via adaptive neural networks," *Engineering Science and Technology, an International Journal*, vol. 35, p. 101259, 2022.

[31] S. Jung and S. S. Kim, "Control Experiment of a Wheel-Driven Mobile Inverted Pendulum Using Neural Network," *IEEE Transactions on Control Systems Technology*, vol. 16, no. 2, pp. 297-303, 2008, doi: 10.1109/TCST.2007.903396.

[32] J. S. Noh, G. H. Lee, H. J. Choi, and S. Jung, "Robust control of a mobile inverted pendulum robot using a RBF neural network controller," *2008 IEEE International Conference on Robotics and Biomimetics*, pp. 1932-1937, 2009, doi: 10.1109/ROBIO.2009.4913296.

[33] W. Junfeng and Z. Wanying, "Design of fuzzy logic controller for two-wheeled self-balancing robot," in *Proceedings of 2011 6th International Forum on Strategic Technology*, vol. 2, pp. 1266-1270, 2011, doi: 10.1109/IFOST.2011.6021250.

[34] J. Wu, W. Zhang, and S. Wang, "A Two-Wheeled Self-Balancing Robot with the Fuzzy PD Control Method," *Mathematical Problems in Engineering*, vol. 2012, p. 469491, 2012, doi: 10.1155/2012/469491.

[35] K. Nader and D. Sarsri, "Modelling and Control of a Two-Wheel Inverted Pendulum Using Fuzzy-PID-Modified State Feedback," *Journal of Robotics*, vol. 2023, p. 4178227, 2023, doi: 10.1155/2023/4178227.

[36] C. H. Huang, W. J. Wang, and C. H. Chiu, "Design and Implementation of Fuzzy Control on a Two-Wheel Inverted Pendulum," *IEEE Transactions on Industrial Electronics*, vol. 58, no. 7, pp. 2988-3001, 2011, doi: 10.1109/TIE.2010.2069076.

[37] T. Zhao, Q. Yu, S. Dian, R. Guo, and S. Li, "Non-singleton General Type-2 Fuzzy Control for a Two-Wheeled Self-Balancing Robot," *International Journal of Fuzzy Systems*, vol. 21, no. 6, pp. 1724-1737, 2019, doi: 10.1007/s40815-019-00664-4.

[38] Y. Zhang, L. Zhang, W. Wang, Y. Li, and Q. Zhang, "Design and Implementation of a Two-Wheel and Hopping Robot With a Linkage Mechanism," *IEEE Access*, vol. 6, pp. 42422-42430, 2018, doi: 10.1109/ACCESS.2018.2859840.

[39] V. Klemm *et al*., "Ascento: A Two-Wheeled Jumping Robot," *2019 International Conference on Robotics and Automation (ICRA)*, pp. 7515-7521, 2019, doi: 10.1109/ICRA.2019.8793792.

[40] H. Zhou, X. Li, H. Feng, J. Li, S. Zhang, and Y. Fu, "Model Decoupling and Control of the Wheeled Humanoid Robot Moving in Sagittal Plane," *2019 IEEE-RAS 19th International Conference on Humanoid Robots (Humanoids)*, pp. 1-6, 2019, doi: 10.1109/Humanoids43949.2019.9035069.

[41] S. Wang *et al.*, "Balance Control of a Novel Wheel-legged Robot: Design and Experiments," *2021 IEEE International Conference on Robotics and Automation (ICRA)*, pp. 6782-6788, 2021, doi: 10.1109/ICRA48506.2021.9561579.

[42] C. Zhang, T. Liu, S. Song, and M. Q. . -H. Meng, "System Design and Balance Control of a Bipedal Leg-wheeled Robot," *2019 IEEE International Conference on Robotics and Biomimetics (ROBIO)*, pp. 1869-1874, 2019, doi: 10.1109/ROBIO49542.2019.8961814.

[43] F. Raza and M. Hayashibe, "Towards Robust Wheel-Legged Biped Robot System: Combining Feedforward and Feedback Control," *2021 IEEE/SICE International Symposium on System Integration (SII)*, pp. 606-612, 2021, doi: 10.1109/IEEECONF49454.2021.9382678.

[44] J. Dong, R. Liu, B. LU, X. Guo, and H. Liu, "LQR-based Balance Control of Two-wheeled Legged Robot," *2022 41st Chinese Control Conference (CCC)*, pp. 450-455, 2022, doi: 10.23919/CCC55666.2022.9902200.

[45] Y. Xin, H. Chai, Y. Li, X. Rong, B. Li, and Y. Li, "Speed and Acceleration Control for a Two Wheel-Leg Robot Based on Distributed Dynamic Model and Whole-Body Control," in *IEEE Access*, vol. 7, pp. 180630-180639, 2019, doi: 10.1109/ACCESS.2019.2959333.

[46] V. Klemm *et al*., "LQR-Assisted Whole-Body Control of a Wheeled Bipedal Robot With Kinematic Loops," in *IEEE Robotics and Automation Letters*, vol. 5, no. 2, pp. 3745-3752, 2020, doi: 10.1109/LRA.2020.2979625.

[47] S. Xin and S. Vijayakumar, "Online Dynamic Motion Planning and Control for Wheeled Biped Robots," *2020 IEEE/RSJ International Conference on Intelligent Robots and Systems (IROS)*, pp. 3892-3899, 2020, doi: 10.1109/IROS45743.2020.9340967.

[48] H. Chen, B. Wang, Z. Hong, C. Shen, P. M. Wensing, and W. Zhang, "Underactuated Motion Planning and Control for Jumping With Wheeled-Bipedal Robots," *IEEE Robotics and Automation Letters,* vol. 6, no. 2, pp. 747-754, 2021, doi: 10.1109/lra.2020.3047787.

[49] T. Guo *et al*., "Design and dynamic analysis of jumping wheel-legged robot in complex terrain environment," *Frontiers in Neurorobotics*, vol. 16, p. 1066714, 2022.

[50] H. G. Lee, "Linearization of Nonlinear Control Systems," *Linearization of Nonlinear Control Systems*, pp. 1-589, 2022.